



	<b>Experiment title:</b> Solid state reaction of polymorphic RE <sub>2</sub> (MoO <sub>4</sub> ) <sub>3</sub> family monitored by X ray thermodiffractometry	<b>Experiment number:</b> 25-01 954
<b>Beamline:</b> BM25	<b>Date of experiment:</b> from: 23/7/2015 (8.00 h) to: 27/7/2015 (8.00 h)	<b>Date of report:</b> 3/7/2016
<b>Shifts:</b> 12	<b>Local contact(s):</b> Eduardo Salas	<i>Received at ESRF:</i>

**Names and affiliations of applicants** (\* indicates experimentalists):

Cristina González-Silgo (Main Proposer). Universidad de La Laguna \*

Candelaria Guzmán-Afonso. Universidad de La Laguna

Manuel Eulalio Torres. Universidad de La Laguna \*

Nanci Sabalisk. Universidad de La Laguna \*

Daniel Ramos-Hernández Universidad de La Laguna \*

Javier López-Solano. Universidad de La Laguna\*

Elena Cedeiras. Universidad de Barcelona \*

Emilio Matesanz. Universidad Complutense de Madrid

Juan Rodríguez-Carvajal. ILL \*

Jesús Iván da Silva González. ISIS Neutron Facility, STFC, UK. \*

**Report:**

**BACKGROUND.** The RE<sub>2</sub>(MoO<sub>4</sub>)<sub>3</sub> family is a fascinating group of compounds which includes an unusual number of polymorph materials with optical, ferroelastic-ferroelectric and electric transport properties which make them useful in diverse technological fields [1]. This rich polymorphism is also made evident under changes of pressure and temperature. No less than ten different crystal structures are known to exist for these compounds from room temperature to their respective melting points, and from 0 GPa to their pressure induced amorphization [2]. This makes them unique as flexible structures, and their study may help to develop new concepts about the physics of phase transitions and amorphization processes under high pressures, as well as related physical properties. At room temperature, and depending on the ionic radii and the synthesis conditions, all the known structures of this family belong to three different polytypes without any symmetry relation among them: the so called “modulated scheelites” for lighter rare earths (La<sub>2</sub>(MoO<sub>4</sub>)<sub>3</sub> [3] and α-Eu<sub>2</sub>(WO<sub>4</sub>)<sub>3</sub> phases [4]), “ferroelectric-paraelectric phases” for RE with intermediate ionic radii (β'-Gd<sub>2</sub>(MoO<sub>4</sub>)<sub>3</sub> and β-Gd<sub>2</sub>(MoO<sub>4</sub>)<sub>3</sub>, respectively [5]), and “negative thermal expansion phases” (γ-Sc<sub>2</sub>(WO<sub>4</sub>)<sub>3</sub> phase [6]) for the heavier RE. We are interested in completing the phase diagram (ionic radii–temperature – pressure) given by Bixner for this family [1] and clarifying the role of the thermal treatment (used in the sample preparation) in the sequence of phase transitions and reversibility observed by monitoring (using XRD in polycrystalline samples) their solid state reaction and following several heating and cooling thermal cycles.

**EXPERIMENTAL.** Samples were measured in the BM25A (ESRF, Grenoble). We established a compromise between obtaining a good resolution (angular range was measured between  $2\theta=4^\circ$  to  $15$  or  $30^\circ$ ), maximizing the number of diffractograms at different temperatures and providing enough time for the measurement of each diffractogram; Therefore the heating rate was not too fast (between  $3^\circ\text{C}/\text{min}$  and  $10^\circ\text{C}/\text{min}$ , excluding the quenching and each diffractogram was measured during  $\sim 15$  minutes). As it can be seen, all samples could not be measured in the same conditions due to the short time, in total, around 100 diffractograms were measured. The wavelength (0.6502 Angstroms) was obtained by verifying the calibrated values with reference to the Si {111} lattice spacing. The temperature was calibrated from  $25^\circ\text{C}$  to  $1000^\circ\text{C}$  collecting data each  $100^\circ\text{C}$ , in a heating process, by using a hot gas blower. Quartz glass capillary with 0.3 mm in diameter was filled with the polycrystalline reference standard of Si. The peak 111 was selected between  $2\theta=11.8$  and  $12.0^\circ$ . Starting samples were the  $\text{MoO}_3$  and  $\text{RE}_2\text{O}_3$  (RE=Nd, Sm, Eu, Gd, Dy and Ho) oxides in order to complete the solid state reaction of most of the rare earth trimolibdates. Note that starting oxides for the synthesis of  $\text{Pr}_2(\text{MoO}_4)_3$  and  $\text{Tb}_2(\text{MoO}_4)_3$ , which belong to this series of lanthanides, do not have the same stoichiometry, thus, these compounds were not studied. Similar experimental conditions to the standard reference were used for our sample. The experiment consisted in a first heating process where the reaction occurred, until around  $1000^\circ\text{C}$ . After that, a cooling process and several new cycles of heating and cooling were measured, in order to determine the complete sequence of phase transitions. Below, we detail the programming of measurements for 12 shifts: 23/07/2015 (08:00) – 27/07/2015 (08:00).

- **From 23 to 24/07/2015:** 1) Standard calibration. 2)  $\text{Nd}_2(\text{MoO}_4)_3$  solid state reaction: heating process ( $3^\circ\text{C}/\text{min}$ ) from room temperature to  $900^\circ\text{C}$ , around 40 diffractograms were measured. An important temperature gradient was detected, these diffractograms shown several phases collected at different temperatures. The hot air blower area for the sample was increased and the problem was solved. 3)  $\text{Nd}_2(\text{MoO}_4)_3$  cooling-heating cycle ( $10^\circ\text{C}/\text{min}$ ):  $900-736-654-736-900^\circ\text{C}$ . 4)  $\text{Nd}_2(\text{MoO}_4)_3$  quenching from  $900^\circ\text{C}$  to  $25^\circ\text{C}$ .

- **From 24 to 25/07/2015:** 1)  $\text{Nd}_2(\text{MoO}_4)_3$  was measured at  $572^\circ\text{C}$ ,  $654^\circ\text{C}$  and  $695^\circ\text{C}$  (heating rate:  $10^\circ\text{C}/\text{min}$ ). 2)  $\text{Sm}_2(\text{MoO}_4)_3$  solid state reaction: heating process ( $3^\circ\text{C}/\text{min}$ ) from room temperature to  $900^\circ\text{C}$ , around 30 diffractograms were measured. 3)  $\text{Sm}_2(\text{MoO}_4)_3$  cooling-heating cycle ( $10^\circ\text{C}/\text{min}$ ):  $900-572-900^\circ\text{C}$ , around 10 diffractograms were measured. 4)  $\text{Sm}_2(\text{MoO}_4)_3$  quenching from  $25^\circ\text{C}$  to  $900^\circ\text{C}$ . 5)  $\text{Sm}_2(\text{MoO}_4)_3$  was measured at  $572^\circ\text{C}$ ,  $645^\circ\text{C}$ ,  $695^\circ\text{C}$  and  $25^\circ\text{C}$  using a heating and cooling rate of  $10^\circ\text{C}/\text{min}$ .

- **From 25 to 26/07/2015:** 1)  $\text{Dy}_2(\text{MoO}_4)_3$  was measured at  $25^\circ\text{C}$ ,  $900^\circ\text{C}$  and at  $25^\circ\text{C}$  using a heating and a cooling rate of  $10^\circ\text{C}/\text{min}$ . 2)  $\text{Ho}_2(\text{MoO}_4)_3$  was measured at  $900^\circ\text{C}$  after a very fast heating, after that it was measured two times at  $900^\circ\text{C}$  waiting for 15 minutes between both measures. 3)  $\text{Eu}_2(\text{MoO}_4)_3$  solid state reaction: heating process ( $10^\circ\text{C}/\text{min}$ ) from room temperature to  $900^\circ\text{C}$ , around 5 diffractograms were measured. 4) Quenching from  $900^\circ\text{C}$  to  $25^\circ\text{C}$ . 5)  $\text{Eu}_2(\text{MoO}_4)_3$  was measured at  $400^\circ\text{C}$ ,  $550^\circ\text{C}$ ,  $700^\circ\text{C}$  and  $800^\circ\text{C}$  with a heating rate of  $10^\circ/\text{min}$ .

- **From 26 to 27/07/2015:** 1)  $\text{Nd}_2(\text{MoO}_4)_3$  was heating from room temperature to  $675^\circ\text{C}$  ( $10^\circ\text{C}/\text{min}$ ) and a diffractogram was measured at this temperature, these measurements correspond to the so-called “repeated experiment”. 2)  $\text{Gd}_2(\text{MoO}_4)_3$  solid state reaction: heating process ( $10^\circ\text{C}/\text{min}$ ) from room temperature to  $900^\circ\text{C}$ , around 15 diffractograms were measured. 3)  $\text{Gd}_2(\text{MoO}_4)_3$ , the temperature was decreased from  $900^\circ\text{C}$  to  $25^\circ\text{C}$  with a cooling rate of  $10^\circ\text{C}/\text{min}$ . Diffractograms were measured at  $900^\circ\text{C}$ ,  $818^\circ\text{C}$ ,  $695^\circ\text{C}$ ,  $450^\circ\text{C}$  and at  $25^\circ\text{C}$ . 4)  $\text{Eu}_2(\text{MoO}_4)_3$ , starting from the alpha-phase at room temperature. The temperature was increased with a heating rate of  $5^\circ/\text{min}$  until  $900^\circ\text{C}$ , 6 diffractograms were measured. 5)  $\text{Eu}_2(\text{MoO}_4)_3$  was cooled at the same rate until  $25^\circ\text{C}$ , 6 diffractograms were measured. 4) and 5) correspond to the so called “last experiment”.

**ANALYSIS OF DATA.** All diffractograms have been visualized with WINPLOTR [7] where the different phases were detected by visual inspection. In the Figure 1 (left), monitored solid state reaction is shown for  $\text{Nd}_2(\text{MoO}_4)_3$ , starting from  $\text{Nd}_2\text{O}_3$  and  $\text{MoO}_3$  oxides (in red at room temperature).  $\text{La}_2(\text{MoO}_4)_3$  can be identify from  $695^\circ\text{C}$  (in yellow), the  $\beta$ -phase is clear at  $900^\circ\text{C}$  (in pink). In Figure 1 (right) we represent some diffractograms obtained from cooling-heating cycles. In red we represent the  $\beta$ -phase at  $900^\circ\text{C}$  after the first heating. In blue the  $\text{La}_2(\text{MoO}_4)_3$  phase is shown at  $645^\circ\text{C}$  after the first cooling. In yellow is shown the beta phase at  $900^\circ\text{C}$  after the second heating. In green is shown the  $\beta$  All diffractograms have been visualized with

WINPLOTR [7] where the different phases were detected by visual inspection. In the Figure 1 (left), monitored solid state reaction is shown for  $\text{Nd}_2(\text{MoO}_4)_3$ , starting from  $\text{Nd}_2\text{O}_3$  and  $\text{MoO}_3$  oxides (in red at room temperature).  $\text{La}_2(\text{MoO}_4)_3$  can be identify from 695°C (in yellow), the  $\beta$ -phase is clear at 900°C (in pink). In Figure 1 (right) we represent some diffractograms obtained from cooling-heating cycles. In red we represent the  $\beta$ -phase at 900°C after the first heating. In blue the  $\text{La}_2(\text{MoO}_4)_3$  phase is shown at 645°C after the first cooling. In yellow is shown the beta phase at 900°C after the second heating. In green is shown the  $\beta$ -phase at room temperature after the quenching. In pink we represent the  $\text{La}_2(\text{MoO}_4)_3$  phase after the third heating.

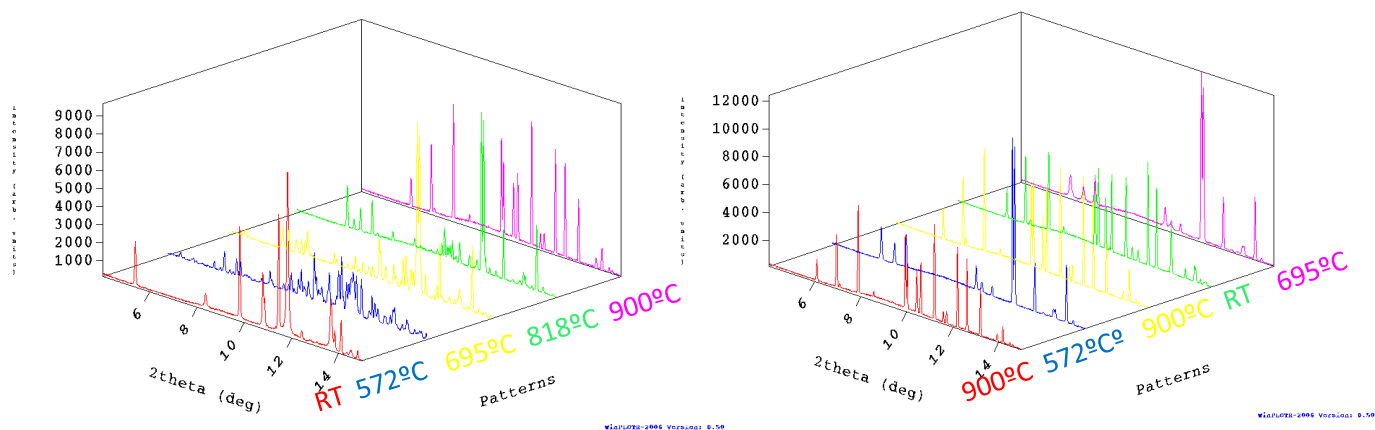


**Figure 1.** Selected diffractograms of monitored solid state reaction where  $\text{Nd}_2(\text{MoO}_4)_3$  was obtained (left). Selected diffractograms measured in several cooling-heating cycles, including a quenching (right).

In Figure 2 (left), the monitored solid state reaction is shown for  $\text{Sm}_2(\text{MoO}_4)_3$ , starting from  $\text{Sm}_2\text{O}_3$  and  $\text{MoO}_3$  oxides (in red at room temperature).  $\alpha$ -phase can be identified from 695°C (in yellow), the  $\beta$ -phase is clear at 900°C (in pink). In Figure 2 (right) we represent some diffractograms obtained from cooling-heating cycles. In red we represent the  $\beta$ -phase at 900°C after the first heating. In blue the  $\alpha$ -phase is shown at 572°C after the first cooling. In yellow is shown the  $\beta$ -phase at 900°C after the second heating. In green is shown the  $\beta$ -phase at room temperature after the quenching. In pink is represented the  $\alpha$ - phase after the third heating.

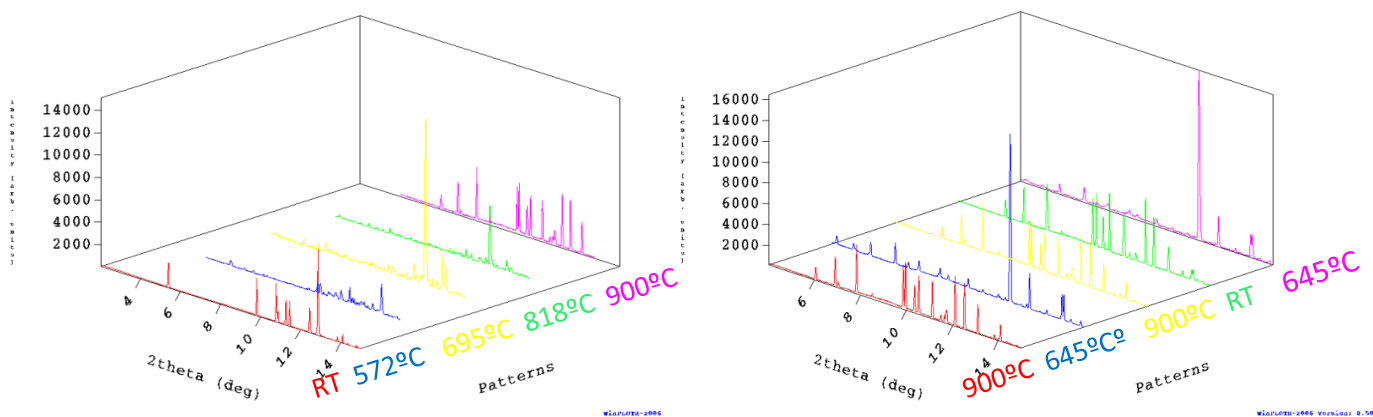


**Figure 2.** Selected diffractograms of the monitored solid state reaction where  $\text{Sm}_2(\text{MoO}_4)_3$  was obtained (left). Selected diffractograms measured in several cooling-heating cycles, including a quenching (right).

The solid state reaction and the  $\alpha$ - $\beta$  phase transition is similar in  $\text{Eu}_2(\text{MoO}_4)_3$  and  $\text{Gd}_2(\text{MoO}_4)_3$ , however we could not visualize the  $\alpha$  phase in the following cooling-heating cycles. In figure 3 we show the “last experiment” performed for  $\text{Eu}_2(\text{MoO}_4)_3$ , starting from the phase alpha (in red), reaching the  $\beta$ -phase at 900°C (in olive). After cooling, at 490°C (in green) it is possible to detect some peaks belonging to the  $\alpha$ -phase which are kept at room temperature (in pink).

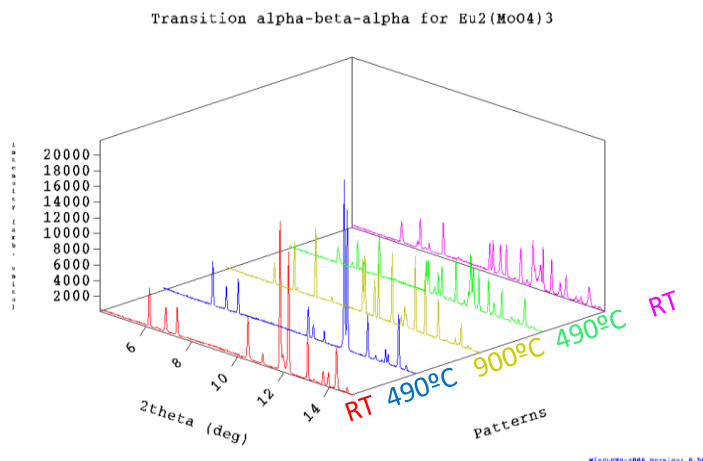
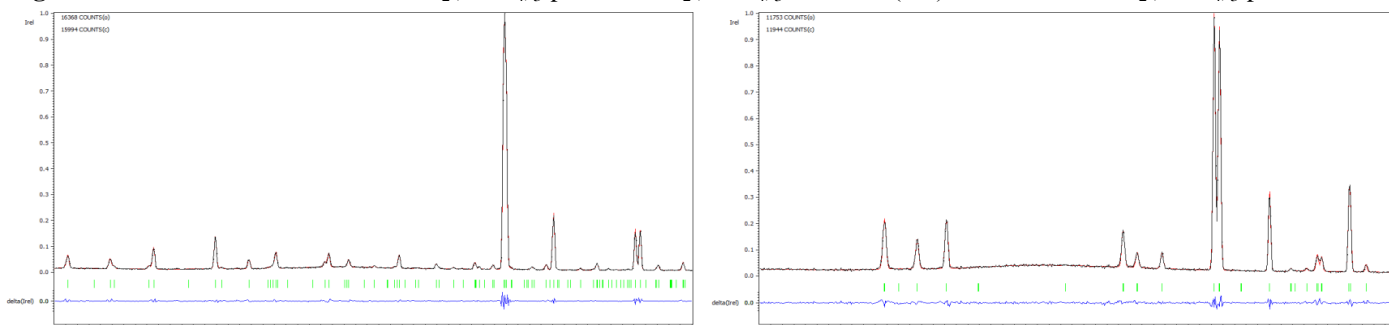


**Figure 3.** Heating-cooling cycle for  $\text{Eu}_2(\text{MoO}_4)_3$

The Le Bail refinements were performed with JANA [8] in order to confirm the pure phases of modulated scheelites:  $\text{La}_2(\text{MoO}_4)_3$  for  $\text{Nd}_2(\text{MoO}_4)_3$  and  $\alpha\text{-Eu}_2(\text{WO}_4)_3$  for  $\text{Sm}_2(\text{MoO}_4)_3$ ,  $\text{Eu}_2(\text{MoO}_4)_3$  and  $\text{Gd}_2(\text{MoO}_4)_3$  (Figure 4). Selected ferroelectric  $\beta'$ -phases at room temperature and paraelectric  $\beta$ -phase at  $900^\circ\text{C}$  were refined for all compounds (Figure 5).

**Figure 4.** Le Bail refinement for the  $\text{La}_2(\text{MoO}_4)_3$ -phase of  $\text{Nd}_2(\text{MoO}_4)_3$  at  $645^\circ\text{C}$  (left) and for the  $\alpha\text{-Sm}_2(\text{MoO}_4)_3$  phase at  $695^\circ\text{C}$ .



Observed data are in black, calculated data are in red and differences are the lower trace, in blue. Bars in green indicate de Bragg positions.

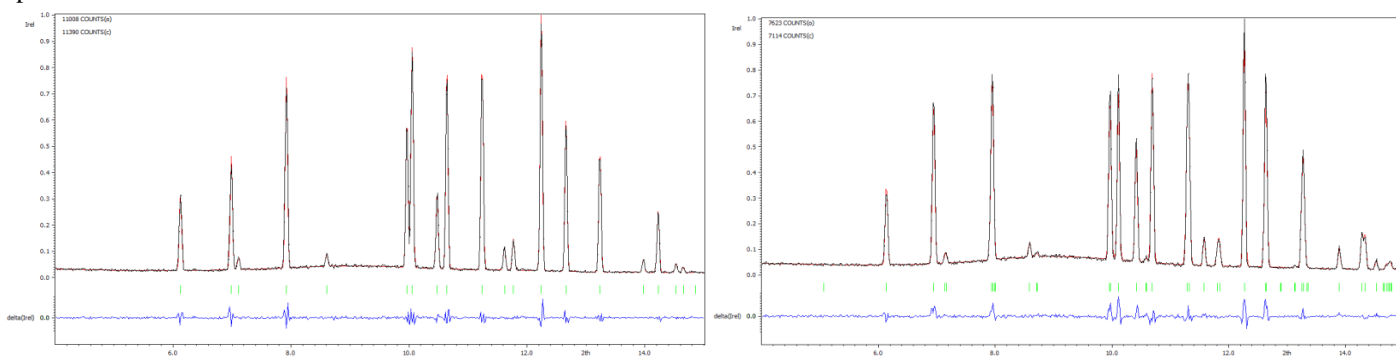


**Figure 5.** Le Bail refinement for the  $\beta$ -paraelectric phase of  $\beta\text{-Eu}_2(\text{MoO}_4)_3$  at  $900^\circ\text{C}$  (left) and for the  $\beta'$ -ferroelectric phase of  $\text{Sm}_2(\text{MoO}_4)_3$ , at room temperature. Observed data are in black, calculated data are in red and differences are the lower trace, in blue. Bars in green indicate de Bragg positions.

Moreover we have refined by the Le Bail algorithm some diffractograms in order to detect mixed phases during the solid state reaction or during the thermal cycles. In Figure 6 (left), we show the mix of  $\alpha$  and  $\beta$ -phases obtained at room temperature for  $\text{Eu}_2(\text{MoO}_4)_3$  in the so-called “last experiment”. These last data were collected by decreasing the heating rate because, following the same protocol used for  $\text{Nd}_2(\text{MoO}_4)_3$  and  $\text{Sm}_2(\text{MoO}_4)_3$ , the  $\alpha$ - $\beta$  and  $\beta$ - $\alpha$  phase transitions were not detected. In Figure 6 (right) it is shown the mix of  $\text{La}_2(\text{MoO}_4)_3$  and  $\alpha$ -phases, collected in the so-called “repeated experiment”. These measurements were performed because, during the first solid state reaction, a gradient of temperature on the sample let to many

mixed phases in each diffractogram, including the starting oxides; thus, we could not distinguish both modulated scheelite phases.

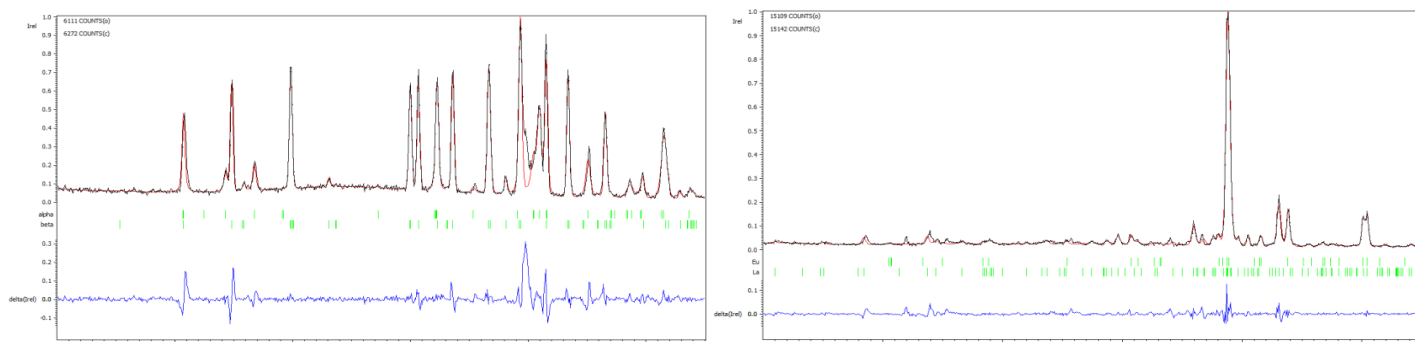


**Figure 6.** Le Bail refinement for the alpha and beta phases of  $\text{Eu}_2(\text{MoO}_4)_3$  at  $297^\circ\text{C}$  (left) and for the alpha and  $\text{La}_2(\text{MoO}_4)_3$  phases of  $\text{Nd}_2(\text{MoO}_4)_3$  at  $695^\circ\text{C}$ . Observed data are in black, calculated data are in red and differences are the lower trace, in blue. Bars in green indicates de Bragg positions for the phases  $\alpha$  (up) and  $\beta$  (down) phases of  $\text{Eu}_2(\text{MoO}_4)_3$  (left) and for the phases  $\alpha$  and  $\text{La}_2(\text{MoO}_4)_3$  of  $\text{Nd}_2(\text{MoO}_4)_3$  (right).

**RESULTS.** The  $\text{La}_2(\text{MoO}_4)_3$  phase and the  $\alpha$ -phase are formed around  $800^\circ\text{C}$  for  $\text{Nd}_2(\text{MoO}_4)_3$  and for Sm, Eu and Gd trimolybdates respectively. It is observed that these modulated scheelites are obtained at high temperature when the ionic radius of the lanthanide is increased. This is a result predicted by some authors but the solid state reactions have never been monitored by X ray diffraction. The  $\text{La}_2(\text{MoO}_4)_3$ - $\beta$  and  $\alpha$ - $\beta$  transitions undergo before  $850^\circ\text{C}$ , as it can be observed from the diagram of phases given by Bixer [1]. During the first cooling, the  $\beta$ - $\alpha$  and  $\beta$ - $\text{La}_2(\text{MoO}_4)_3$  phase transitions were detected for  $\text{Sm}_2(\text{MoO}_4)_3$  and  $\text{Nd}_2(\text{MoO}_4)_3$  respectively at around  $700^\circ\text{C}$ . Also, during the first heating, the  $\alpha$ - $\beta$  and  $\text{La}_2(\text{MoO}_4)_3$ - $\beta$  phase transition were detected at the same temperature. These reversible transitions, without an appreciable thermal hysteresis, have been observed for the first time. This is an important result because the  $\beta$  and modulated scheelite phases are not related by symmetry, thus, a non-abrupt first order phase transition occurs. For  $\text{Eu}_2(\text{MoO}_4)_3$  and  $\text{Gd}_2(\text{MoO}_4)_3$  the same result is expected but the heating and cooling rate must be slower and the transition temperature decreases. An important result, which has never been described, was the  $\beta$ - $\alpha$  (or  $\text{La}_2(\text{MoO}_4)_3$ ) transition undergoing around  $700^\circ\text{C}$ , when the  $\beta$ -phase was obtained by quenching from  $900^\circ\text{C}$  to room temperature and the temperature was increased. Nd trimolybdate could be refined, using the Le Bail algorithm, with the modulated scheelite structure ( $\text{La}_2(\text{MoO}_4)_3$  structure,  $C2/c$  space group) with different ordering of RE and stoichiometric vacancies than that of the Sm, Eu, Gd trimolybdates, which could be refined with the so-called  $\alpha$ -phase (with the  $\text{Eu}_2(\text{WO}_4)_3$  structure and also the  $C2/c$  space group, but with a volume three times smaller). For all compounds, the tetragonal paraelectric phase of  $\text{Gd}_2(\text{MoO}_4)_3$  ( $\beta$ -phase) at high temperature ( $P4_21m$  space group) and the ferroelectric phase ( $\beta'$ -phase) at room temperature ( $Pba2$  space group) could be refined too. Another important result was the detection of a mixture of the phases  $\alpha$  and  $\text{La}_2(\text{MoO}_4)_3$  for the  $\text{Nd}_2(\text{MoO}_4)_3$  during the solid state reaction (“repeated experiment”). This can be connected with the incommensurable phase observed for  $\text{Pr}_2(\text{MoO}_4)_3$  [9]. Finally, as it was expected, the  $\alpha$ -phase was not detected for  $\text{Ho}_2(\text{MoO}_4)_3$  and we had no time to study the  $\gamma$ - $\beta$  and  $\beta$ - $\gamma$  phase transition, in order to complete our recent work [10].

**Acknowledges.** The authors are grateful to ESRF (Grenoble, France) and the Ministerio de Ciencia e Innovación of Spain (MAT2013-43319-P) for the financial support.

## References.

- [1] L.H. Brixner, J.R. Barkley, W. Jeitschko *Handbook on the Physic and Chemistry of Rare Earths*, North-Holland Publishing Co., Amsterdam, 1979.
- [2] M. Maczka *et al. Progress in Materials* **57**, 1335-1381 (2012).
- [3] W. Jeitschko. *Acta Cryst. B* **29**, 2074-2081 (1973).
- [4] H.D. Templeton and A. Zalkin, *Acta Cryst. B* **16**, 762 (1963).
- [5] W. Jeitschko. *Acta Cryst B*, **28**, 60-76. (1972).
- [6] N. Imanaka *et al.*, *Chem. Mater.* **12**, 1910-1913, (2000).
- [7] WinPlotR. <https://www.ill.eu/sites/fullprof/>.
- [8] JANA2006, version 10/06/2016, <http://jana.fzu.cz>.
- [9] D. Logvinovich *et al. Inorg Chem.* **49.4** 1587-94 (2010).
- [10] C. González-Silgo *et al. Powder Diffraction* **28**, 833-840 (2013).